Testing spinless-boson-parent models for anomalous $l^+l^-\gamma$ events

H. Baer
CERN, Theory Division, CH-1211 Genève 23, Switzerland

K. Hagiwara
DESY, Theory Group, D-2000 Hamburg-52, Federal Republic of Germany

J. Ohnemus
Physics Department, University of Wisconsin, Madison, Wisconsin 53706
(Received 30 November 1984)

Models with production of a heavy ($\simeq m_Z$) spinless boson and its subsequent radiative decay into a lepton pair and a photon are studied, with cuts appropriate to the CERN $p\bar{p}$ collider experiments. Dalitz plots for the $l^+l^-\gamma$ final state and their projections are shown; the agreement with the data is generally slightly better than the radiative-Z-decay models but is not sufficient to account for the characteristics of the three observed events.

I. INTRODUCTION

The observation of three $l^+l^-\gamma$ ($l=e$ or μ) events with very high energy noncollinear photons by the UA1 (Refs. 1 and 2) and UA2 (Ref. 3) collaborations at the CERN $p\bar{p}$ collider has led to various speculations on their origin. In a previous paper[4] the models with radiative Z-boson decay were critically studied and it was shown that none of the models provides a likely explanation of the observed events. The most characteristic feature of the observed events is that in all three cases, one of the $l\gamma$ systems has a very small invariant mass, which the models we examined fail to reproduce.

Subsequently, we learned about the possibility[5-8] that the observed lepton pair and a photon may not come from the Z boson, but from a spinless boson, which we hereafter denote ϕ, whose mass is accidentally near m_Z. A common feature of these models is, as emphasized by Matsuda and Matsuoka,[6] that the photon tends to be collinear with one of the charged leptons because of angular-momentum conservation. This can lead to an enhancement in the small-lepton-photon-invariant-mass region.

In this paper we examine the consequences of these models quantitatively and show their Dalitz plots, l^+l^- and $l\gamma$ invariant-mass distributions, and γ transverse-momentum distributions. We find that the enhancement of the cross section in the small-$l\gamma$-invariant-mass region obtained in these models is not sufficiently large to account for the characteristics of the three data points.

Unless otherwise stated, the parameters and the final-state cuts we impose are identical to those we employed in Ref. 4. We set $m_\phi = m_Z$ ($=94$ GeV) for definiteness.

We sketch briefly the models[5-8] in Sec. II, and comparisons with the data are made in Sec. III.

II. MODELS

Since the production and decay parts of the cross section factorize for a spinless boson, we can discuss each property separately.

A. Production

Several different mechanisms have been proposed for ϕ production. In all models,[5-8] the underlying chiral symmetry is supposed to suppress direct coupling of ϕ to a massless-fermion pair. Hence we do not expect the subprocess $q\bar{q}\to\phi$ to have a substantial contribution in $p\bar{p}$ collision. If ϕ has a charge-conjugation parity $C=+$, then the subprocess[8]

$$g+g\to\phi \tag{1}$$

can be important. If ϕ has $C=-$ (Ref. 7), then the following $2\to2$ subprocesses can have significant contributions:

$$q+\bar{q}\to\phi+g\ , \tag{2a}$$

$$q+g\to\phi+q\ , \tag{2b}$$

$$g+g\to\phi+g\ . \tag{2c}$$

Subprocesses (2a) and (2b) have been considered explicitly by Holdom.[5] It is also possible[6] that ϕ is produced via radiative Z decay

$$q+\bar{q}\to Z\to\phi+\gamma \tag{3}$$

if m_ϕ is slightly lower than m_Z such that the emitted photon is sufficiently soft and remains undetected.

Since our primary concern is the $l^+l^-\gamma$ final state, the various production mechanisms affect our results only through the p_T distribution of the ϕ boson. The sub-

processes (2) naturally lead to a harder p_T spectrum due to one-jet emission. Even in the subprocesses (1) and (3), however, hard fusion would typically lead to multiple gluon bremsstrahlung. It would not be easy to distinguish between different mechanisms by looking into the hadronic activity accompanying ϕ production. On the other hand, we know from the p_T distributions of the observed $l^+l^-\gamma$ events that the distributions cannot be too different from other $Z\to l^+l^-$ events.

In the following numerical calculation, we show only the results obtained by the $gg\to\phi$ mechanism [Eq. (1)]. We have checked the sensitivity of our results to different production mechanisms by introducing a Gaussian p_T distribution of ϕ with $\langle p_T\rangle=10$ GeV and also by repeating the calculation with the subprocess (3); only in this latter case we set $m_\phi=m_Z-5$ GeV. We have found no significant deviation in either case apart from the slight shift in the photon p_T distribution and the trivial kinematical constraint imposed by the choice of a different m_ϕ in the latter case.

Before we proceed to the ϕ radiative-decay properties, two comments are in order.

There exists a strong constraint[9] on the ϕ decay width Γ_ϕ if the gluon fusion subprocess (1) is the main production mechanism. By assuming that the three observed $l^+l^-\gamma$ events come via $\phi\to Z_v\gamma$ transition (Z_v denotes virtual Z boson), we estimate from Fig. 1 of Ref. 9 that the ϕ width is bounded as

$$\Gamma_\phi\simeq\frac{1\text{ GeV}}{B(\phi\to gg)B(\phi\to Z_v\gamma)}>4\text{ GeV}\ , \tag{4}$$

where the lower bound is taken when $B(\phi\to gg)\simeq B(\phi\to Z_v\gamma)\simeq\frac{1}{2}$, that is, when the two branching fractions are comparable and all other decay fractions [e.g., $B(\phi\to\gamma\gamma)$] are negligible. In our numerical calculation, we set $\Gamma_\phi=5$ GeV; doubling this value does not lead to any significant changes. With too large a width, we lose an enhancement in the $l^+l^-\gamma$ production cross section near m_ϕ, which gives a nontrivial constraint in this model.

Second, if we literally use the dimension-7 local operators presented in Ref. 5 to calculate the ϕ-production cross section via the subprocesses (2a) and (2b), we encounter a very hard p_T distribution for ϕ. Typically, we obtain $\langle p_T\rangle\simeq 50$ GeV in $p\bar{p}$ collisions at $\sqrt{s}=540$ GeV. This is due to the singular high-energy behavior of the subprocess cross sections,

$$\hat{\sigma}\to\frac{\hat{s}^2}{\Lambda^6} \tag{5}$$

with Λ being the mass scale of the new interaction. This does not necessarily rule out the possibility of the contact interactions because of the low statistics of the data and also because the nonlocality or form factor of the interaction can easily tame the hard p_T spectrum; the appearance of the form-factor damping may even be natural because the mass scale Λ was estimated[5] to be as low as 100 GeV.

B. Decay

In both of the models with ϕ production via subprocesses (1) and (3), $\phi\to l^+l^-\gamma$ decays should occur via the strong $\phi Z\gamma$ coupling which is needed to obtain large $B(\phi\to Z_v\gamma)$ in the former case or large $B(Z\to\phi\gamma)$ in the latter case. In momentum space the gauge-invariant $\phi Z\gamma$ vertices are

$$\Gamma^{\mu\nu}(p,q,k)=i\frac{f_P}{\Lambda}\epsilon^{\mu\nu\lambda\sigma}q_\lambda k_\sigma+i\frac{f_S}{\Lambda}[k^\mu q^\nu-(kq)g^{\mu\nu}]\ , \tag{6}$$

where μ and ν denote Z and γ polarization indices, and p, q, and k are the four-momenta of the ϕ, Z, and γ, respectively; $f_P=0$ for the scalar ϕ and $f_S=0$ for pseudoscalar ϕ. The differential decay distributions for $\phi\to\bar{l}l\gamma$ then reads for pseudoscalar ϕ,

$$\frac{d\Gamma}{dx\,dy}=\frac{m_\phi{}^3\alpha[(g_V^l)^2+(g_A^l)^2]}{64\pi^2\Lambda^2}\times\frac{f_p(x)^2x(y^2+z^2)}{(m_Z{}^2/m_\phi{}^2-x)^2+(m_Z\Gamma_Z/m_\phi{}^2)^2}\ , \tag{7}$$

where we have introduced the scaling variables

$$\begin{aligned}x&=(p_l+p_{\bar{l}})^2/m_\phi{}^2\ ,\\ y&=(p_l+p_\gamma)^2/m_\phi{}^2\ ,\\ z&=(p_{\bar{l}}+p_\gamma)^2/m_\phi{}^2\ ,\end{aligned} \tag{8}$$

and g_V^l and g_A^l are the vector and axial-vector couplings of the Z—lepton-pair vertices as defined in Ref. 4. The form factor f_p can in general be a function of x. In the $m_\phi=m_Z$ and $\Gamma_Z/m_Z=0$ limit, we find a simple normalized distribution

$$\frac{1}{\Gamma}\frac{d\Gamma}{dx\,dy}=B(\phi\to\bar{l}l\gamma)\frac{9x(y^2+z^2)}{(1-x)^2} \tag{9}$$

for $f_P(x)=$constant. A scalar ϕ gives an identical distribution.

The decay $\phi\to l^+l^-\gamma$ can also occur via contact four-point interactions:[5]

$$\Gamma^\mu(p,l,\bar{l},\gamma)=i\frac{g_S}{\Lambda^3}e[q^\mu\not{k}-(qk)\gamma^\mu]+i\frac{g_P}{\Lambda^3}e\epsilon^{\mu\nu\rho\sigma}k_\rho q_\sigma\gamma_\nu+\frac{g_P'}{\Lambda^3}e[(p_l-p_{\bar{l}})^\mu\not{k}-(kp_l-kp_{\bar{l}})\gamma^\mu]\gamma_5\ , \tag{10}$$

where g_S, g_P, and g_P' are in general functions of x and y, $g_S=0$ for pseudoscalar ϕ and $g_P=g_P'=0$ for scalar ϕ. The differential decay distribution for scalar ϕ then reads

$$\frac{d\Gamma}{dx\,dy}=\frac{m_\phi{}^7\alpha}{64\pi^2\Lambda^6}g_S(x,y)^2x(y^2+z^2)\ . \tag{11}$$

For constant form factors we obtain the normalized decay distribution

$$\frac{1}{\Gamma}\frac{d\Gamma}{dx\,dy}=B(\phi\to\bar{l}l\gamma)30x(y^2+z^2) \tag{12}$$

for both scalar and pseudoscalar. The distributions (9) and (12) differ from each other only by the Z-propagator factor $(1-x)^{-2}$.

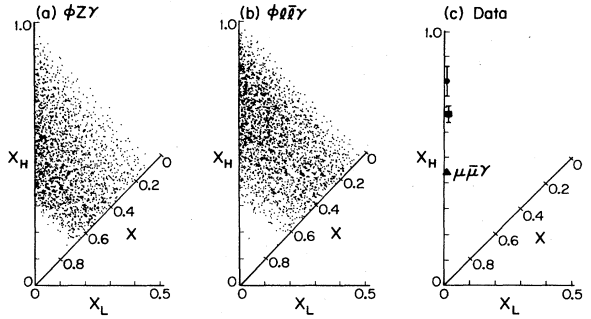

FIG. 1. Dalitz plots for the process $p\bar{p}\to l^+l^-\gamma+$anything, for spinless-boson-parent models with cuts as described in the text. The models illustrated are (a) the $\phi Z\gamma$ coupling model and (b) the contact $\phi l\bar{l}\gamma$ coupling model. The Dalitz-plot locations of data points are also shown (c) from Refs. 1 and 3 ($e^+e^-\gamma$) and Ref. 2 ($\mu^+\mu^-\gamma$).

III. RESULTS

A. Dalitz plots

Figure 1 illustrates the Dalitz plots of the $l^+l^-\gamma$ expected in the $\phi Z\gamma$ coupling model (a), and in the contact $\phi l\bar{l}\gamma$ coupling model (b), along with the corresponding three data points (c). The horizontal, vertical, and diagonal axes measure, respectively.

$$x_L=[\text{lower } m(l\gamma)^2]/m(l^+l^-\gamma)^2\,,$$
$$x_H=[\text{higher } m(l\gamma)^2]/m(l^+l^-\gamma)^2\,, \qquad (13)$$
$$x=m(l^+l^-)^2/m(l^+l^-\gamma)^2\,,$$

which satisfy the relation $x_L+x_H+x=1$. Three data points are shown as a solid circle,[1] a solid square,[3] and a solid triangle.[2]

If we compare Figs. 1(a) and 1(b) with the corresponding Dalitz plots for the anomalous-Z-radiative-decay models (Fig. 2 of Ref. 4), we find enhancement in the density in the small-x_L region. However, the density in the small-x_L region is much weaker than the corresponding one for the standard model [Fig. 1(a) of Ref. 4]. Between the two models considered in this paper, the $\phi Z\gamma$ coupling model tends to have slightly more events in the high x than the $\phi l\bar{l}\gamma$ coupling model and hence the former model predictions are more sensitive to the experimental cuts.

B. Invariant-mass distributions

In Figs. 2(a), 2(b), and 2(c), we show three projections of the Dalitz plots but on a linear scale in invariant masses, $m(l^+l^-)$, lower $m(l\gamma)$, and higher $m(l\gamma)$, respectively. The standard-model distributions[4] are also shown as a reference.

In the $m(l^+l^-)$ distribution, the difference between the $\phi Z\gamma$ model and the direct-coupling model can be understood qualitatively as a Z-boson-propagator effect. The difference is, however, not as spectacular as suggested from the difference in the two distributions, because the high-$m(l^+l^-)$ region (large-x region) tends to be cut off

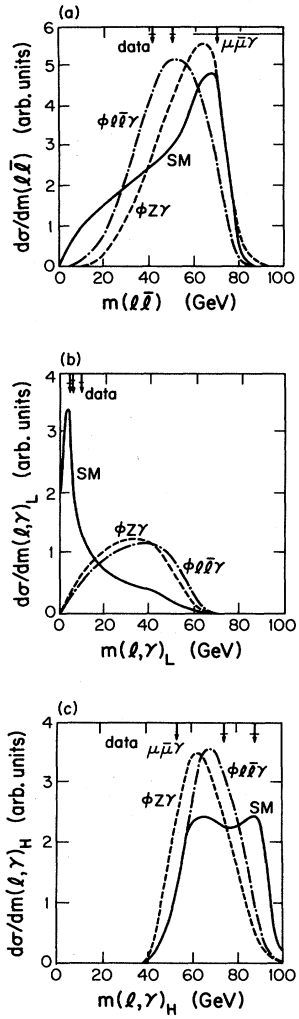

FIG. 2. Invariant-mass distributions for the process $p\bar{p}\to l^+l^-\gamma+$anything, for the models of Fig. 1 and the standard model with cuts as described in the text: (a) $m(l^+l^-)$, (b) lower $m(l\gamma)$, and (c) higher $m(l\gamma)$.

by the experimental acceptance cut for the γ transverse momentum.

The discrepancy between these models and the three data points can most clearly be seen in the $m(l\gamma)_L$ distribution shown in Fig. 2(b). Here all three data points lie below $m(l\gamma)_L\simeq 10$ GeV, while both models fail to have sufficient population there. The enhancement which appeared in

$$x_L=m(l\gamma)_L{}^2/m(l^+l^-\gamma)^2$$

is so weak that it virtually disappears in the linear $m(l\gamma)_L$ distributions due to the Jacobian factor, $m(l\gamma)_L$. Introduction of a mild form factor cannot improve the situation significantly. Dissimilarity of these models to the standard-model prediction is also most clear in this projection. It would still be fair to say, however, that the models with a spinless-boson parent[5–8] studied in this paper have a better chance to survive compared to the Z-boson-parent models examined in Ref. 4.

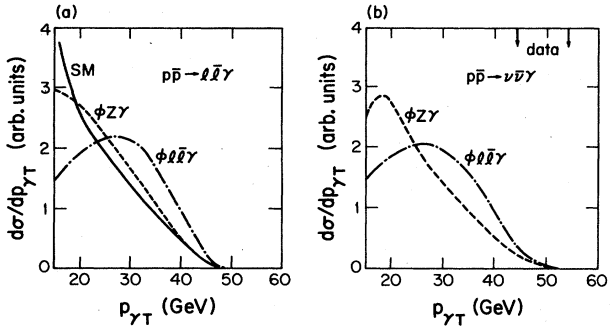

FIG. 3. Photon transverse-momentum distribution for the models of Fig. 1 and the standard model with cuts as described in the text: (a) $p\bar{p}\to l^+l^-\gamma+$anything and (b) $p\bar{p}\to\nu\bar{\nu}\gamma+$anything.

C. Photon transverse-momentum distribution

Figure 3(a) shows the distribution in $p_{\gamma T}$, the photon momentum transverse to the beam axis. The published data have not quoted the $p_{\gamma T}$ values. As we stressed in Ref. 4, the $p_{\gamma T}$ distribution is useful to examine in a model-independent way whether the $l^+l^-\gamma$ events and the reported[10] two missing-p_T+"photon" events have a common origin.

The decays $\phi\to\nu\bar{\nu}\gamma$ are naturally expected in the $\phi Z\gamma$ model with a rate 5.9 times larger than the $\phi\to e^+e^-\gamma$ rate. In the direct $\phi l\bar{l}\gamma$ coupling model of Holdom,[5] we still expect the $\phi\nu\bar{\nu}\gamma$ coupling to exist at some level, but with an unpredictable rate.

We show in Fig. 3(b) the $p_{\gamma T}$ distributions for the $\phi\to\nu\bar{\nu}\gamma$ decay in the two models; the only difference between the calculations of Figs. 3(a) and 3(b) is that we naturally remove all the cuts in lepton momenta in the latter. Two UA1 data points[10] are also shown. We find that the spinless-boson-parent models tend to have softer $p_{\gamma T}$ distributions than the Z-boson-parent models [compare Fig. 3(b) with Fig. 5(b) of Ref. 4]. This tendency is stronger in the $\phi Z\gamma$ model, which makes it very unlikely that the model can account for the missing-p_T+"photon" events.

IV. CONCLUSION

The consequences of the spinless-boson-parent model for the anomalous $l^+l^-\gamma$ events have been studied in detail with appropriate experimental cuts. Our conclusion remains unchanged from the one obtained in the analysis of the Z-boson-parent models:[4] none of the models studied so far gives a satisfactory explanation for the simple fact that all three observed events have very small lower $m(l\gamma)$.

Note added. After essentially completing this work, we learned that K. Hikasa arrived at the same conclusion independently.[11]

ACKNOWLEDGMENTS

The authors wish to thank V. Barger for his interest and many fruitful discussions. They also thank K. Hikasa for useful comments on the manuscript.

[1]UA1 collaboration, G. Arnison *et al.*, Phys. Lett. **126B**, 398 (1983); **135B**, 250 (1984).
[2]UA1 collaboration, G. Arnison *et al.*, Phys. Lett. **147B**, 241 (1984).
[3]UA2 collaboration, P. Bagnaia *et al.*, Phys. Lett. **129B**, 130 (1983).
[4]V. Barger, H. Baer, and K. Hagiwara, Phys. Rev. D **30**, 1513 (1984).
[5]B. Holdom, Phys. Lett. **143B**, 241 (1984).
[6]M. Matsuda and T. Matsuoka, Phys. Lett. **144B**, 443 (1984).
[7]V. Gupta and K. V. L. Sarma, Phys. Lett. **144B**, 447 (1984).
[8]W. J. Marciano, Phys. Rev. Lett. **53**, 975 (1984).
[9]V. Barger, H. Baer, and K. Hagiwara, Phys. Lett. **146B**, 257 (1984).
[10]UA1 collaboration, G. Arnison *et al.*, Phys. Lett. **139B**, 115 (1984).
[11]K. Hikasa, Phys. Lett. **153B**, 108 (1984).